ELSEVIER

Catalysis Today 47 (1999) 73–82

CATALYSIS TODAY

Preparation and characterization of $LaCrO_3$ and Cr_2O_3 methane combustion catalysts supported on $LaAl_{11}O_{18}$- and Al_2O_3-coated monoliths

Marcus F.M. Zwinkels[1], Oliver Haussner, P. Govind Menon, Sven G. Järås*

Kungl Tekniska Högskolan (Royal Institute of Technology), Department of Chemical Engineering and Technology – Chemical Technology, S-100 44 Stockholm, Sweden

Abstract

A series of $LaAl_{11}O_{18}$- and Al_2O_3-supported $LaCrO_3$ and Cr_2O_3 combustion catalysts was prepared. Different active phase–support combinations were prepared and applied to cordierite monoliths. The washcoat materials were aged in flowing humid air at temperatures between 1100°C and 1400°C, after which they were characterized by BET, XRD, TPR, and EDS. The monolith catalysts were evaluated in methane combustion. The presence of an active phase retarded sintering of the Al_2O_3 support, whereas the active phase slightly decreased the thermal stability of $LaAl_{11}O_{18}$. X-ray measurements revealed extensive interaction between support and active phase in the washcoat materials. A substituted perovskite, $LaCr_{1-x}Al_xO_3$, is proposed to be formed in nearly all samples containing both lanthanum and chromium. The accessibility of chromium decreased rapidly after aging. The activities of the Al_2O_3-supported catalysts were higher than of those supported on $LaAl_{11}O_{18}$, which was related to the higher surface area of the former.

Keywords: Chromium; Combustion catalyst; Co-precipitation; Deposition–precipitation; Impregnation; Lanthanum hexa-aluminate; Perovskite; Support–active phase interaction; Thermal stability

1. Introduction

Thermal stability of combustion catalysts is regarded as one of the outstanding hurdles before catalytic combustion technology can be further developed and commercialized [1,2]. This thermal stability comprises not only the surface area stability of the support but also the chemical stability and sintering resistance of the support–active phase system. Two approaches may be taken for achieving the highest possible thermal stability for the support–active phase system.

The first approach is the incorporation of the active phase in the support lattice, yielding a so-called active support. The most successful example of an active support in catalytic combustion was developed by Arai and co-workers, [3] i.e. manganese-substituted barium hexa-aluminate $BaMnAl_{11}O_{19-\alpha}$ and was recently demonstrated in an actual gas turbine combustor [4].

Another approach is combining a highly thermostable support and a thermostable active phase that are compatible with each other. This approach implies various requirements on the active material:

*Corresponding author. Tel.: +46-8-790-8917; fax: +46-8-108-579.

[1]Present address: AB Sandvik Coromant R&D, Materials and Processes 12680 Stockholm, Sweden

0920-5861/99/$ – see front matter
PII: S0920-5861(98)00284-3

1. The active material should not increase the sintering rate of the support material.
2. A stable dispersion on the support should be achieved.
3. The active material should not react with the support to give a new inactive phase, a phenomenon well-known for Al_2O_3-supported transition metal catalysts which may react to form spinels [5,6].
4. The active material must have a sufficiently low vapor pressure under anticipated operating conditions.

Various examples of this second approach have been reported in the literature. Copper oxide on different supports was reported as promising, e.g. lanthanum-stabilized alumina [7] and $ZnAl_2O_4$ [8]. Marti et al. [9] studied $La_{0.8}Sr_{0.2}MnO_{3+x}$ supported on $LaAlO_3$ and $LaAl_{11}O_{18}$, and on different spinels MAl_2O_4 (M=Co, Mg, Ni) [10]. Marti et al. observed a higher activity of the supported perovskites than of the bulk material as a result of an increased dispersion of the active phase due to the application on a support. Jeong Kwon et al. [11] recently reported on various transition metal oxides, supported on a mixed lanthanum–aluminum oxide. They found chromium oxide to be the most interesting of the studied metal oxides, since it did not affect the sintering behavior of the support and maintained a constant surface composition up to 1400°C. Collongue et al. [12] incorporated chromium in a thermostable perovskite lattice, i.e. $LaCrO_3$, and investigated both the bulk and supported oxides.

We have presently chosen the second approach, with the current study focusing on the suitability of supported $LaCrO_3$ and Cr_2O_3 as combustion catalysts. The supports used are $LaAl_{11}O_{18}$ and commercial alumina. This work focuses on the effect of the active material on the thermal stability of the support and the occurrence of solid state reactions between the support and the active material. Finally, different materials are deposited on cordierite honeycombs for the evaluation of methane combustion activity.

2. Experimental

2.1. Catalyst preparation

2.1.1. Preparation of $LaAl_{11}O_{18}$

The preparation route was similar to the one reported by Marti et al. [9]; a mixed lanthanum–aluminum hydroxide was prepared by a coprecipitation method. Lanthanum nitrate ($La(NO_3)_3{\cdot}6H_2O$, Riedel-de Haën, >99%) and aluminum nitrate ($Al(NO_3)_3{\cdot}9H_2O$, Riedel-de Haën, >98%) were used as the starting materials. A mixed solution of these nitrates (total cation concentration 1 M) was added dropwise to stirred aqueous ammonia (pH 8.5–9), yielding a mixed lanthanum–aluminum hydroxide precipitate. The pH in the precipitation flask was kept constant by a controlled dropwise supply of ammonia (Labassco, 25 wt%). After precipitation was completed the mixture was stirred for 20 min and the precipitate was aged overnight at room temperature. The precipitate was then centrifuged and washed with deionized water three times and dried at 200°C overnight. Finally, the material was calcined at 500°C and at 1000°C for 4 h each, after which it was ground.

2.1.2. Application of the active phase

Incipient wetness impregnation and deposition–precipitation were used to apply the active phase on the support. These two methods were chosen since they might result in different degrees of interaction between the active phase and the support. Moreover, deposition–precipitation might yield a higher dispersion than incipient wetness. When impregnating to incipient wetness, a suitable amount of metal (Cr or La/Cr) nitrates was dissolved in that amount of water which corresponded to the pore volume of the support. The deposition–precipitation method has previously been reported for copper [7] and nickel catalysts [13]. We applied this method for supported Cr_2O_3 catalysts according to the following route. The support powder was suspended in a solution of chromium nitrate ($Cr(NO_3)_3{\cdot}9H_2O$, Merck, >98%) and urea (H_2NCONH_2, Riedel-de Haën, 99.5%). The molar ratio of Cr to urea was about 1–9. This high ratio was needed since urea forms a complex with chromium that hinders precipitation of the hydroxide. The suspension was continually stirred and slowly heated to 90°C, which initiated decomposition of the urea, liberating ammonia homogeneously throughout the suspension. Air was bubbled through the solution during this process. After precipitation of chromium hydroxide on the support, the solution was aged overnight, after which it was centrifuged.

The alumina-supported catalysts were prepared from commercial boehmite (Pural SCF 55, Condea Chemie GmbH) with a surface area of 253 m^2/g.

The materials thus prepared were dried at 200°C overnight and calcined at 500°C for 4 h. The loading of active material was 10 wt% in the case of Cr_2O_3 and 10 or 30 wt% in the case of $LaCrO_3$.

2.1.3. Preparation of monolithic catalysts

Washcoats were applied onto cordierite monoliths by a dip-coating procedure described in more detail elsewhere [14,15]. The powder, to be deposited on the monolith, was dispersed in water, giving a slurry. This slurry was stirred vigorously for 2 h after which it was ball-milled overnight. Monolith samples with a cell density of 400 cpsi, of suitable size for the activity tests, were immersed in the slurry, after which they were withdrawn slowly. The excess slurry remaining in the channels after withdrawal was forced out by blowing air through the monoliths. The samples were then dried at 200°C. This procedure was repeated several times to give a washcoat loading of approximately 15% of the total weight. The catalyst samples thus prepared were calcined at 500°C and 1000°C for 4 h each. Part of the slurry was saved, and dried and calcined in the same way as the monoliths, for aging tests and characterization.

2.2. Characterization and activity tests

A series of supported Cr_2O_3 and $LaCrO_3$ washcoat materials was aged in a 10 vol% steam in air flow at temperatures between 1100 and 1400°C to study the thermal stability of the support–active phase system. The details of this treatment are given in [16]. The materials are denoted in the following way: *active material/support-comment*. Active material may be C (Cr_2O_3) or LC ($LaCrO_3$), support may be A (Al_2O_3) or LHA ($LaAl_{11}O_{18}$). The comment may be DP (deposition–precipitation) or IW (incipient wetness) for the Cr_2O_3 samples and 10 or 30 for the $LaCrO_3$ samples, which in that case denotes the weight percentage of the active phase. Thus LC/A-30 represents 30 wt% $LaCrO_3/Al_2O_3$. In all cases but the Cr_2O_3/Al_2O_3 catalysts, samples were taken from the slurries used for the washcoating of monoliths, described in Section 2.1.3. The Cr_2O_3/Al_2O_3 sample was taken from the washcoat precursor material before ball-milling. The washcoat materials studied are summarized in Table 1.

The phase compositions of the calcined and aged samples were investigated with powder X-ray diffraction using a Siemens Diffraktometer 5000 operating with the following parameters: Cu K_α radiation, 30 mA, 40 kV, Ni filter, 2θ scanning range 10–85°, and scan step size 0.02. Phase identification was made using the reference database, supplied with the equipment. BET surface area and pore volume were determined by nitrogen adsorption using a Micromeritics ASAP 2000. Samples were outgassed in vacuum at 250°C for at least 3 h before the adsorption measurements. Qualitative analysis of the chromium content of the samples was made by energy dispersive X-ray spectrometry (EDS) using a LINK QX2000 unit. Atomic absorption spectrophotometry, using a Perkin-Elmer 1100B, was in some cases applied to confirm the EDS data.

Temperature-programmed reduction (TPR) of the powder samples was performed using a Micromeritics TPD/TPR 2900, equipped with a thermal conductivity detector. The amount of sample was 300–500 mg, the flow rate of the 10 vol% H_2/Ar gas mixture was approximately 50 ml/min, and the heating rate was 10°C/min.

The activities of the monolith catalysts were tested in a ceramic tubular reactor, placed in a temperature-programmed furnace. The air was preheated before

Table 1
Prepared washcoat materials

Material ID	Target composition	Application active material
C/A-DP	10 wt% Cr_2O_3/Al_2O_3	Deposition–precipitation
LC/A-30	30 wt% $LaCrO_3/Al_2O_3$	Incipient wetness impregnation
C/LHA-DP	10 wt% $Cr_2O_3/LaAl_{11}O_{18}$	Deposition–precipitation
C/LHA-IW	10 wt% $Cr_2O_3/LaAl_{11}O_{18}$	Incipient wetness impregnation
LC/LHA-10	10 wt% $LaCrO_3/LaAl_{11}O_{18}$	Incipient wetness impregnation
LC/LHA-30	30 wt% $LaCrO_3/LaAl_{11}O_{18}$	Incipient wetness impregnation

mixing with CH_4, just upstream of the catalyst. The total gas flow was 5.7 N l/min with a calculated CH_4 concentration of 2 vol%, giving a space velocity of about 46 000 h^{-1}. All experiments were conducted at atmospheric pressure. The heating rate was 2°C/min. The combustion products were analyzed on-line using a Balzers QMG 421C quadrupole mass spectrometer. A typical activity evaluation consisted of a test run, as described above, followed by aging in situ in dry flowing air at 1100°C for 12 h, after which a second test run was done.

3. Results and discussion

3.1. Sintering of supported $LaCrO_3$ and Cr_2O_3 samples

The surface areas for a series of powder samples after calcination at 1000°C and subsequent aging at various temperatures are given in Fig. 1(a) and (b), and compared with the areas of the supports alone.

Fig. 1(a) clearly shows the strong decrease in surface area of the commercial alumina between 1000°C and 1100°C, related to the transition to the stable α-phase. The continued decrease at higher temperatures is due to crystal growth and densification. The presence of chromium (C/A-DP) apparently retards the sintering of alumina, a rapid decrease of surface area is observed between 1100°C and 1200°C instead. The $LaCrO_3/Al_2O_3$ sample (LC/A-30) exhibits a much more moderate decrease in surface area than the other two samples. The presence of lanthanum is likely to stabilize the surface of Al_2O_3, as was previously reported by many authors, e.g. [17,18,19]. This is confirmed by the X-ray results, given in Section 3.2.

The $LaAl_{11}O_{18}$-supported materials had lower surface area than the support itself, which is shown in Fig. 1(b). The differences for the calcined materials (1000°C) are mainly due to the application of the active phase itself. Of the Cr_2O_3 materials, the surface area of the sample prepared by deposition–precipitation (C/LHA-DP) approached the support quite closely, whereas the surface area of the sample prepared by incipient wetness (C/LHA-IW) was 50–60% lower than that of the support at all temperatures. This difference is not in line with the recently reported results by Jeong Kwon et al. [11]. They found the surface area of a 10 wt% Cr_2O_3 catalyst, applied on a La/Al complex oxide by impregnation, to be somewhat higher than that of the support. They explained their observation by the stable dispersion of Cr_2O_3 on the support, which retarded sintering. It needs to be mentioned that their high-temperature treatment implied aging for only 2 h and that no details were given on the aging environment. On the other hand, our XRD measurements showed significant solid-state interaction between Cr_2O_3 and the support.

The deposition–precipitation sample not only had a higher surface area than the incipient wetness sample, the pore volume was also much higher for the former, e.g. 0.096 and 0.044 ml/g, respectively, at 1100°C. This may be an indication of a better Cr_2O_3 dispersion in the deposition–precipitation sample compared to the other material.

The supported $LaCrO_3$ samples showed a lower surface area than the support at all temperatures. The sample with the highest loading (LC/LHA-30) had the lowest surface area, but the difference between the two $LaCrO_3$ samples decreased with rising temperature. At the highest temperatures, the levels of the surface area approached that of the incipient wetness Cr_2O_3 sample.

3.2. Crystal structure

A summary of the XRD results is given in Table 2, showing the phases observed in the calcined and aged washcoat samples, as well as in the support materials. Both Cr_2O_3 and $LaCrO_3$ retarded the formation of the α-phase, when supported on Al_2O_3, cf. C/A-DP and LC/A-30, respectively. Cr_2O_3 only shifted the phase transition to higher temperatures, but $LaCrO_3$ interacted more strongly with the Al_2O_3 support. At 1200°C and higher temperatures a $LaAl_{11}O_{18}$ phase was observed, formed by the reaction between lanthanum and Al_2O_3. Moreover, a perovskite phase was formed, which is discussed below. The formation of these new phases is most likely the cause for the higher surface area stability of LC/A-30, as compared to that of the support, cf. Fig. 1(a); the stabilizing effect of lanthanum on Al_2O_3 is well known [17–19]. Beguin et al. [19] detected the $LaAlO_3$ perovskite in lanthanum-modified Al_2O_3, after aging at 1050°C and 1220°C. They attributed the stabilization to this perovskite phase, which they believed was formed from

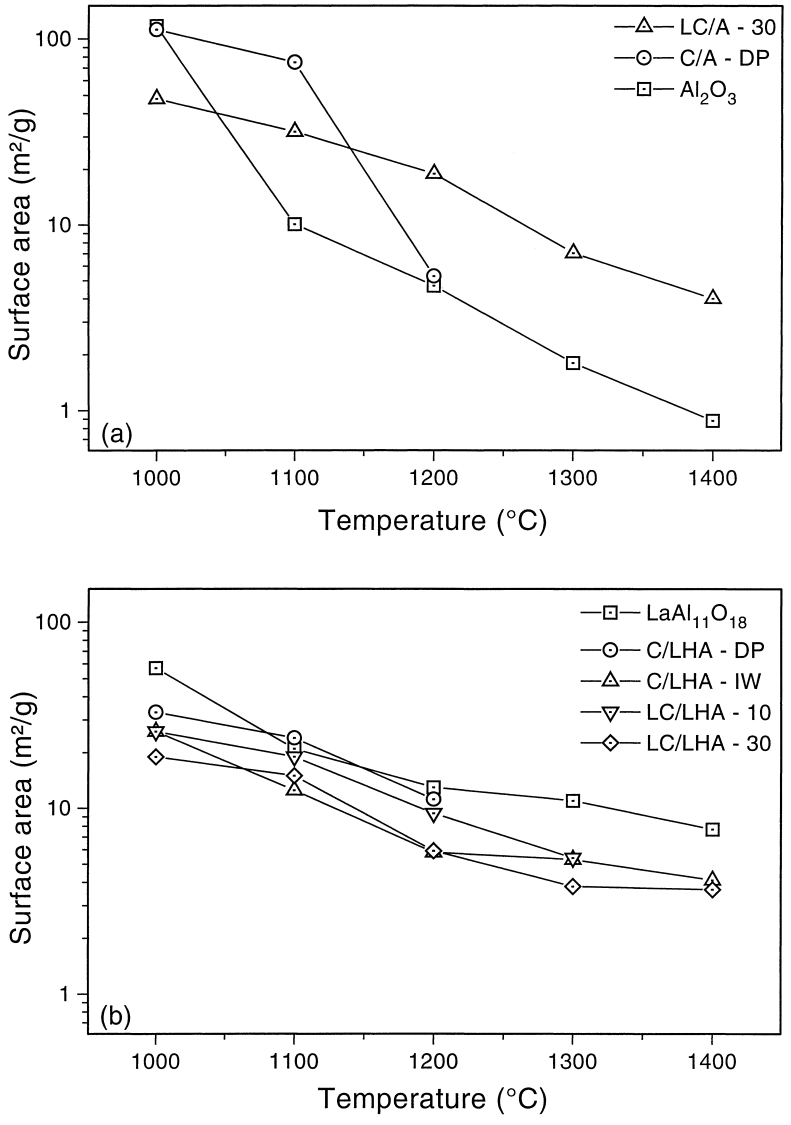

Fig. 1. Surface areas of Al_2O_3-supported (a) and $LaAl_{11}O_{18}$-supported (b) catalysts after aging in a 10 vol% H_2O in air flow at various temperatures for 16 h. Results for the supports are given for comparison. Figures at 1000°C denote surface areas after calcination in air.

lanthanum and reactive surface aluminum ions. At the highest temperature, $LaAl_{11}O_{18}$ was also observed, which was assumed to be a product of reaction between $LaAlO_3$ and Al_2O_3.

The $LaAl_{11}O_{18}$-supported Cr_2O_3 samples showed sharp $LaCrO_3$ perovskite peaks after calcination at 1000°C. The amorphous lanthanum–aluminum mixed oxide contained reactive lanthanum and aluminum ions, which could react with the applied Cr_2O_3. The diffraction patterns of the $LaCrO_3$ sample after calcination depended on the loading of the active phase. The 10 wt% sample (LC/LHA-10) showed sharp perovskite peaks, very close to those of the $LaAlO_3$ reference, whereas the corresponding peaks for the 30 wt% sample (LC/LHA-30) were very close to those of the $LaCrO_3$ reference.

All aged $LaAl_{11}O_{18}$ samples exhibited a more extensive reaction between the support and the active

Table 2
Crystalline phases observed in the washcoat samples after calcination in air (1000°C) and aging at various temperatures in a 10 vol% H_2O in air flow for 16 h

Material ID	Temperature (°C)				
	1000	1100	1200	1300	1400
Al_2O_3	δ, θ, **A**	α	α	α	α
C/A-DP	δ, θ, **A**	δ, θ, **A**	α	α	α
LC/A-30	**LC**, δ	**LCA**	**LCA**, LHA, α	**LCA**, LHA, α	**LCA**, LHA, α
$LaAl_{11}O_{18}$	LA, **A**	**LA**, LHA	**LA**, LHA	**LA**, LHA	**LHA**, LA
C/LHA-DP	**LC**	**LC**	**LCA**, α, LHA	**LCA**, α, LHA	
C/LHA-IW	**LC**	**LCA**, α, LHA	**LCA**, α, LHA	**LCA**, α, LHA	**LCA**, α, LHA
LC/LHA-10	**LA**	**LA**	**LA**, α	**LA**, α, LHA	
LC/LHA-30	LC	**LC**	**LCA**, α	**LCA**, α	**LCA**, α, LHA

Major phases in bold print. Data for the supports [16] are added for reference.
A: amorphous, α, δ, θ: alumina phases, LC: $LaCrO_3$, LA: $LaAlO_3$, LHA: $LaAl_{11}O_{18}$, LCA: $LaCr_{1-x}Al_xO_3$.

phase than the corresponding calcined materials. In all cases, this led to a disturbance of the lanthanum–aluminum ratio in the support, which was shown by the occurrence of unwanted phases, such as α-Al_2O_3.

In the case of the Cr_2O_3 samples, lanthanum reacted first with Cr_2O_3, giving $LaCrO_3$. At higher temperatures aluminum ions were incorporated into this perovskite, forming the substituted perovskite $LaCr_{1-x}Al_xO_3$. This assumption is supported by the XRD findings, represented in Fig. 2. The major perovskite peak was shifted from a position very close to the $LaCrO_3$ reference to a position in-between the $LaCrO_3$ and $LaAlO_3$ references.

The reaction path observed after aging for the $LaAl_{11}O_{18}$-supported $LaCrO_3$ samples depended on the loading of the active phase. The 10 wt% sample

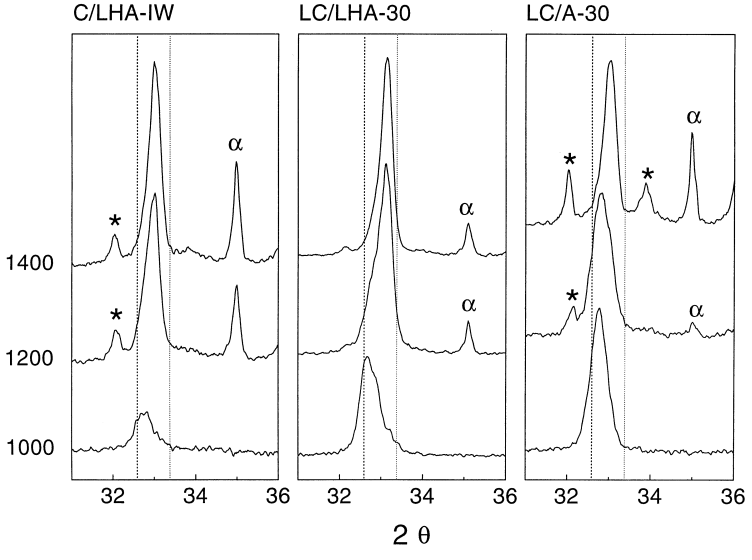

Fig. 2. Details of the X-ray diffraction patterns of three samples taken after calcination (1000°C) in air and aging at 1200°C and 1400°C in 10 vol% H_2O for 16 h. Dashed line: reference peak angle for $LaCrO_3$; dotted line: reference peak angle for $LaAlO_3$; α: α-Al_2O_3; ★: $LaAl_{11}O_{18}$.

showed perovskite peaks close to the $LaAlO_3$ reference at all temperatures. $LaAl_{11}O_{18}$ and α-Al_2O_3 were observed at higher temperatures. The observed main perovskite peaks in both LC/A-30 and LC/LHA-30 shifted from near the $LaCrO_3$ reference to a position between the $LaCrO_3$ and $LaAlO_3$ references, as shown in Fig. 2. This indicates the formation of the substituted perovskite $LaCr_{1-x}Al_xO_3$, as was the case for the $LaAl_{11}O_{18}$-supported Cr_2O_3 samples.

The extensive reactions between active phase and support influenced the crystallization of the support itself. The retarded formation of α-Al_2O_3 in the Al_2O_3-supported samples was already mentioned above. Table 1 clearly shows an increased formation of α-Al_2O_3 in the $LaAl_{11}O_{18}$-supported samples as compared to the support. This is probably due to the disturbance in the lanthanum–aluminum ratio of the support, induced by the reactions between support and active phase. The formation of the target phase of the support, $LaAl_{11}O_{18}$ was retarded due to the interaction with the active phase; in the case of LC/LHA-30, only traces of the target phase were found after 1400°C.

Collongue et al. [12] did not observe a substituted perovskite after aging of their 20 wt% $LaCrO_3/Al_2O_3$ catalyst in a stoichiometric methane–air mixture at 1070°C for 24 h. Perhaps the temperature in their treatment was too low to enable the required solid-phase reaction. Another possibility may be that their procedure for application of the active material involved a sequential application of lanthanum and chromium. This procedure may hinder the diffusion of aluminum ions into the perovskite.

It appears from the above discussion that the solid-state reactions between the support and active phase should be avoided as much as possible, or controlled so that the desired phase composition is eventually obtained. Retardation of such unwanted solid-state reactions may be achieved by applying the active material to a support that has been subjected to thermal treatment at high temperatures. Such a support material already has the desired phase composition, rendering the cations less active, which may retard the solid-state reactions.

3.3. TPR

The chemical nature of the active phase in the prepared washcoat materials was further investigated with temperature-programmed reduction. Fig. 3 shows the reduction profiles of four of the calcined samples. All samples studied exhibited single peaks in the reduction profile between 350°C and 380°C.

The C/A-DP sample showed a peak at 350°C, which was also seen for a comparable sample, prepared by incipient wetness impregnation. The other three sam-

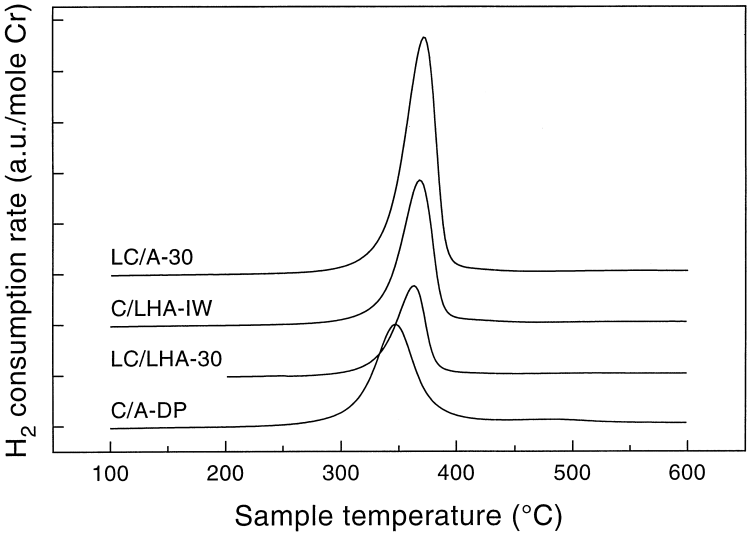

Fig. 3. TPR profiles of four samples after calcination at 1000°C.

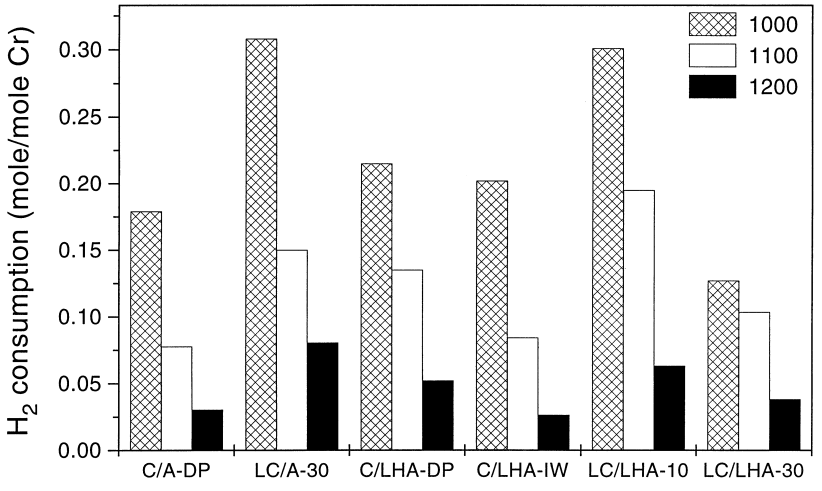

Fig. 4. Hydrogen consumption in TPR of calcined (1000°C) and aged samples. Aging in a 10 vol% H_2O in air flow for 16 h.

ples had peak temperatures between 365°C and 375°C. Chromium was present in a perovskite lattice in these three samples, and was apparently slightly more difficult to reduce than well-dispersed Cr_2O_3 in the C/A-DP sample. The peak temperatures of all samples tended to decrease by 10–20°C due to aging. Other studies on supported chromia catalysts showed peak temperatures of 350°C (Al_2O_3 [20]) and 320°C (La–Al complex oxide [11]); in both cases a single-peak reduction profile was observed. These results are in line with our findings, regarding the fact that Jeong Kwon et al. [11] observed no formation of perovskite in their Cr_2O_3/La–Al oxide catalyst.

The total amount of hydrogen consumed during TPR was calculated by the integration of the profiles. Fig. 4 gives a summary of the hydrogen consumption of all samples during TPR after calcination and aging at 1100°C and 1200°C.

The values for the hydrogen consumption for the calcined materials (1000°C) indicate that the accessibility of the chromium differed strongly between the samples, assuming that a higher consumption implies a better accessibility. The highest values, around 0.30 mol H_2/mol Cr, were obtained for LC/A-30 and LC/LHA-10. LC/LHA-30 displayed a much lower hydrogen consumption, 0.13 mol H_2/mol Cr. The surface area of the $LaAl_{11}O_{18}$ apparently was not high enough to allow a high dispersion of 30 wt% supported perovskite. This assumption is supported by the fact that the surface area of LC/LHA-30 was only 33% of that of the support after calcination. Some smaller pores might have been blocked due to the application of the active phase. The three Cr_2O_3 samples all merely consumed about 0.2 mol H_2/mol Cr after calcination. The lower hydrogen consumption compared to LC/A-30 and LC/LHA-10 is probably related to a lower dispersion of the Cr_2O_3 samples. Encapsulation of the active phase during calcination is not expected, since the support was pre-calcined at the same temperature as the support–active phase system.

All samples displayed a strong decrease in hydrogen consumption as a result of aging. The values after aging at 1200°C varied between 0.025 and 0.075 mol H_2/mol Cr. A combination of support sintering and active phase sintering is assumed to be the cause for these observations. For example, the surface area of the Al_2O_3-supported samples decreased by 90% after aging. The growth of the $LaCr_{1-x}Al_xO_3$ phase, proposed in Section 3.2, in all lanthanum-containing samples should also be detrimental for the accessibility of the chromium.

It could be suggested that the strong decrease in hydrogen consumption was a consequence of chromium loss during aging, due to vaporization [21]. Therefore, a qualitative assessment of the chromium content of the samples was made with EDS, before and after aging at various temperatures. No significant decrease in chromium content due to aging was observed in any of the samples. These results were confirmed by AAS for the Al_2O_3-supported catalysts.

Hence, chromium vaporization can be discarded as a reason for the decrease in hydrogen consumption after aging. The TPR profiles of Cr_2O_3/La–Al complex oxide in the study by Jeong Kwon et al. [11] also indicated a decreasing hydrogen consumption at increasing calcination temperature, without being commented in the paper.

3.4. Activity tests

The activities of cordierite-supported catalysts were measured after calcination, and after aging in situ at 1100°C in dry flowing air for 12 h. The results of the activity tests are shown in Table 3, giving T_{10} and T_{50}, the temperatures needed for 10% and 50% conversion of methane.

The Al_2O_3-supported catalysts were more active than their $LaAl_{11}O_{18}$ counterparts, both before and after aging. However, they lost activity due to aging, which was not the case for the $LaAl_{11}O_{18}$-supported catalysts. The latter had similar values for T_{10} and T_{50} before and after aging.

The lower activity of the $LaAl_{11}O_{18}$-supported catalysts as compared to the Al_2O_3-supported samples is likely to be related to the higher surface area of the latter, cf. Fig. 1. This higher surface area probably favored a high dispersion of the active phase. Besides, in the case of 30 wt% $LaCrO_3$/$LaAl_{11}O_{18}$, small pores may have been blocked by the applied active phase. Moreover, an extensive reaction was observed between the active phase and $LaAl_{11}O_{18}$, already after calcination. The target crystalline hexa-aluminate phase was not formed after calcination at 1000°C [16], and hence the reactive lanthanum and aluminum ions were available for diffusion into a preferred perovskite lattice. Comparing the two $LaAl_{11}O_{18}$-supported Cr_2O_3 samples, incipient wetness yields higher activity than deposition–precipitation. This is probably related to the stronger interaction of C/LHA-DP compared to C/LHA-IW, which was expected (cf. Section 2.1.2).

It needs to be mentioned though that these catalysts were not so active in methane combustion. Especially at higher conversion levels for the least active catalysts, the contribution of homogeneous reactions became significant in the used test equipment. However, the order in activity is the same with respect to T_{10} and T_{50}, and seems thus not to be upset when homogeneous combustion is superimposed on the heterogeneous catalytic reactions.

The low combustion activity may be the result of an insufficient washcoat loading, i.e. 15%. A high washcoat loading was previously demonstrated to favor activity in catalytic combustion [14], and a higher loading could thus give a more fair comparison of the heterogeneous catalytic activity.

4. Conclusions

A series of Al_2O_3- and $LaAl_{11}O_{18}$-supported Cr_2O_3 and $LaCrO_3$ catalysts were compared as to their suitability in combustion applications. Thermal aging in humid air at temperatures anticipated in combustion chambers induced strong interactions between support and active phase. In some cases these reactions had a beneficial effect on the stability of the support–active phase system. $LaCrO_3$ was found to stabilize Al_2O_3, strongly hindering the formation of the undesired α-Al_2O_3. However, it is not clear whether the suggested formation of a substituted perovskite $LaCr_{1-x}Al_xO_3$ was favorable. This perovskite was observed in nearly all sample combinations containing both lanthanum and chromium. In any case, it is desirable to further investigate $LaCr_{1-x}Al_xO_3$ to elucidate the mechanism of its formation and characteristics.

Table 3
Activities for methane combustion for fresh and aged catalysts (aging in situ in flowing dry air at 1100°C for 12 h)

Material ID	$T_{10,fresh}$ (°C)	$T_{10,aged}$ (°C)	$T_{50,fresh}$ (°C)	$T_{50,aged}$ (°C)
C/A-DP	524	542	575	604
LC/A-30	515	542	564	604
C/LHA-DP	582	589	640	640
C/LHA-IW	572	572	611	607
LC/LHA-10	594	587	673	665
LC/LHA-30	567	560	614	608

The $LaAl_{11}O_{18}$-supported catalysts were less active in methane combustion than their Al_2O_3-supported counterparts. Lower surface areas of the former is likely to be the main reason for this observation. The low surface area results in poor dispersion of the active phase, and probably pore blocking due to application of the active phase. A support material with a higher porosity should avoid part of these problems. Sol–gel synthesis should thus be explored further as a method for the preparation of highly homogeneous, highly porous mixed oxides [16].

Moreover, the solid-state reactions between the support and the active phase appeared to be more extensive in the $LaAl_{11}O_{18}$-catalysts, compared to the Al_2O_3-based ones. It is probably beneficial for a stable dispersion of the active material to have a crystalline support with a relatively inactive surface. This was demonstrated by Collongue et al. [12] who supported $LaCrO_3$ on $MgAl_2O_4$. Such a passivated support surface may be achieved by thermal treatment prior to the application of the active phase; this may be a promising approach for achieving higher thermal stability for supported combustion catalysts.

Acknowledgements

This work was supported by NUTEK, The Swedish National Board for Industrial and Technical Development. The authors wish to thank Inga Groth for valuable help with the XRD, EDS and BET analyses.

References

[1] M.F.M. Zwinkels, S.G. Järås, P.G. Menon, T.A. Griffin, Catal. Rev.-Sci. Eng. 35 (1993) 319.
[2] S.T. Kolaczkowski, Trans. IChemE. 73 (1995) 168.
[3] M. Machida, K. Eguchi, H. Arai, J. Catal. 120 (1989) 377.
[4] H. Sadamori, T. Tanioka, T. Matsuhisa, in: H. Arai (Ed.), Proceedings of the Second International Workshop, Catal. Comb., Tokyo, 18–20 April 1994, Catalysis Society of Japan, Tokyo, p. 158.
[5] D.J. Young, P. Udaja, D.L. Trimm, in: B. Delmon, G.F. Froment (Eds.), Catalyst deactivation, Stud. Surf. Sci. Catal. 6 (1980) 331.
[6] P.H. Bolt, M.E. van Ipenburg, J.W. Geus, F.H.P.M. Habraken, MRS Symposium and Proceedings, 344, Materials Research Society, 1994, p. 15.
[7] I.I.M. Tijburg, Ph.D. Thesis, University of Utrecht, 1989.
[8] M.C. Marion, E. Garbowski, M. Primet, J. Chem. Soc., Faraday Trans. 87 (1991) 1795–1800.
[9] P.E. Marti, M. Maciejewski, A. Baiker, in: G. Poncelet, P.A. Jacobs, P. Grange, B. Delmon (Eds.), Preparation of Catalysts VI, Louvain-La-Neuve, 5–8 September, 1994, Elsevier, Amsterdam, p. 617.
[10] P.E. Marti, M. Maciejewski, A. Baiker, Appl. Catal. B 4 (1994) 225.
[11] S. Jeong Kwon, H. Baik-Huon, J. Soon-Yong, K. Jaecheon, L. Jung Min, Microporous Mater. 3 (1995) 657.
[12] B. de Collongue, E. Garbowski, M. Primet, J. Chem. Soc., Faraday Trans. 87 (1991) 2493.
[13] X. Xiaoding, H. Vonk, A. Cybulski, J.A. Moulijn, in: G. Poncelet, P.A. Jacobs, P. Grange, B. Delmon (Eds.), Preparation of Catalysts VI, Louvain-La-Neuve, 5–8 September 1994, Elsevier, Amsterdam, p. 1069.
[14] M.F.M. Zwinkels, S.G. Järås, P.G. Menon, in: G. Poncelet, J. Martens, B. Delmon, P.A. Jacobs, P. Grange (Eds.), Preparation of Catalysts VI, Louvain-La-Neuve, 5–8 September 1994, Elsevier, Amsterdam, p. 85.
[15] M.F.M. Zwinkels, S.G. Järås, P.G. Menon, K.I. Åsen, J. Mater. Sci. 31 (1996) 6345.
[16] M.F.M. Zwinkels, S. Druesne, E. Björnbom, P.G. Menon, S.G. Järås, Ind. Eng. Chem. Res. 37 (1998) 391.
[17] H. Schaper, E.B.M. Doesburg, L.L. van Reijen, Appl. Catal. 7 (1983) 211.
[18] I.I.M. Tijburg, J.W. Geus, H.W. Zandbergen, J. Mater. Sci. 26 (1991) 6479.
[19] B. Beguin, E. Garbowski, M. Primet, Appl. Catal. 75 (1991) 119.
[20] K. Yih-Ming, W. Ben-zu, Appl. Catal. A 114 (1994) 35.
[21] P.M.J.A. Hermans, Z.I. Kolar, F. Kapteijn, J.J.M. de Goeij, J.A. Moulijn, Book of Abstracts, Europacat II, Maastricht, 3–8 September 1995.